

AECL-5552

**ATOMIC ENERGY
OF CANADA LIMITED**



**L'ÉNERGIE ATOMIQUE
DU CANADA LIMITÉE**

IRRADIATION CREEP IN ZIRCONIUM SINGLE CRYSTALS

by

S.R. MACEWEN and V. FIDLERIS

Presented at International Colloquium on Measurement of Irradiation
Enhanced Creep in Nuclear Materials, Petten, Netherlands,
5-6 May 1976

Chalk River Nuclear Laboratories

Chalk River, Ontario

July 1976

ATOMIC ENERGY OF CANADA LIMITED

IRRADIATION CREEP IN ZIRCONIUM SINGLE CRYSTALS

by

S.R. MacEwen and V. Fidleris*

Presented at International Colloquium on Measurement of
Irradiation Enhanced Creep in Nuclear Materials,
Petten, Netherlands, 5-6 May 1976

Materials Science Branch
Chalk River Nuclear Laboratories
Chalk River, Ontario
July 1976

Fluage d'irradiation dans les cristaux uniques de zirconium

par

S.R. MacEwen et V. Fidleris

Présenté au Colloque international de mesure du
fluage d'irradiation dans les matériaux nucléaires,
Petten, Hollande, 5-6 mai 1976

Résumé

Deux cristaux uniques identiques de zirconium en barre cristalline ont fait l'objet d'essais de fluage en réacteur. Les deux spécimens ont été pré-irradiés sous faible contrainte jusqu'à une dose d'environ 4×10^{23} n/m² ($E > 1$ MeV) et ils ont ensuite été chargés jusqu'à 25 MPa. Le premier spécimen a été chargé alors que le réacteur était à pleine puissance et le deuxième au cours d'un arrêt. La contrainte de charge pour les deux cristaux était de plus d'un ordre de grandeur plus petit que celle observée lorsqu'un cristal non irradié identique était chargé sous la même contrainte. On a noté des périodes de fluage primaire pour les deux spécimens après lesquelles la vitesse du fluage a atteint des valeurs presque constantes lorsque le réacteur était en fonctionnement. Durant les arrêts, la vitesse du fluage décroissait rapidement avec le temps.

La microscopie électronique a révélé que les dommages par irradiation comprenaient des boucles de dislocation prismatique ayant approximativement 13.5 nm de diamètre. Des canaux vides, identifiés comme gisant sur (1010) des plans ont également été observés. Les résultats sont commentés en fonction des théories actuelles concernant le fluage d'irradiation à la lumière des microstructures observées.

L'Energie Atomique du Canada, Limitée
Laboratoires Nucléaires de Chalk River
Chalk River, Ontario

Juillet 1976

AECL-5552

ATOMIC ENERGY OF CANADA LIMITED
IRRADIATION CREEP IN ZIRCONIUM SINGLE CRYSTALS

by

S.R. MacEwen and V. Fidleris*

Presented at International Colloquium on Measurement of
Irradiation Enhanced Creep in Nuclear Materials,
Petten, Netherlands, 5-6 May 1976

ABSTRACT

Two identical single crystals of crystal bar zirconium have been creep tested in reactor. Both specimens were pre-irradiated at low stress to a dose of about 4×10^{23} n/m² ($E > 1$ MeV), and were then loaded to 25 MPa. The first specimen was loaded with reactor at full power, the second during a shut-down. The loading strain for both crystals was more than an order of magnitude smaller than that observed when an identical unirradiated crystal was loaded to the same stress. Both crystals exhibited periods of primary creep, after which their creep rates reached nearly constant values when the reactor was at power. During shutdowns the creep rates decreased rapidly with time.

Electron microscopy revealed that the irradiation damage consisted of prismatic dislocation loops, approximately 13.5 nm in diameter. Cleared channels, identified as lying on (10 $\bar{1}$ 0) planes, were also observed. The results are discussed in terms of the current theories for flux enhanced creep in the light of the microstructures observed.

Materials Science Branch
Chalk River Nuclear Laboratories
Chalk River, Ontario

July 1976

IRRADIATION CREEP IN ZIRCONIUM SINGLE CRYSTALS

by

S.F. MacEwen and V. Fidleris

Presented at International Colloquium on Measurement of
Irradiation Enhanced Creep in Nuclear Materials,
Petten, Netherlands, 5-6 May 1976

1. Introduction

The development of a theory for the irradiation enhancement of creep depends on three critical factors. First, one needs to know the nature of the displacement damage: how many point defects are produced per incident particle, how many spontaneously recombine and, therefore, how many become free to diffuse through the lattice to sinks. It may also be important to know how the vacancies and interstitials are distributed immediately after a cascade, before they commence their diffusive processes. Second, one needs to know the origin of the bias which causes the point defects to be partitioned among the various types of sinks present in the crystal. In the absence of a bias all sinks would receive equal fluxes of vacancies and interstitials. If random fluctuations in the arrival rates of the point defects were neglected, no net sink motion would result. Finally, one needs to know how the motion of the sinks can lead to a plastic deformation rate which agrees with experiment not only in magnitude, but also in its temperature, stress, and flux dependencies. The most straightforward assumption is that the strain results directly from the climb of dislocations. Heald and Speight⁽¹⁾, Wolfer and Ashkin^(2,3), and Bullough and Hayns⁽⁴⁾ have recently derived expressions for creep based on the net climb of network dislocations and

growth of prismatic loops. Models based on a combined climb-glide concept have been developed by Nichols⁽⁵⁾, Dollins^(6,7), Gittus^(8,9) and Hesketh⁽¹⁰⁾. Although details of the models differ, it is generally accepted that the rate controlling step is flux enhanced climb, with glide the strain producing mechanism.

The experiments to be described were designed to clarify the last two points. The bias of a particular sink for a particular point defect arises from both the misfit interaction and from the modulus, or inhomogeneity, interaction. If the latter is negligible for a variety of possible reasons, then a neutral or unbiased sink, such as a grain boundary, is required if flux enhanced dislocation climb is to occur. This is not the case if the inhomogeneity interaction is important in determining the bias of a given sink. By creep testing single crystals an important neutral sink, the grain boundary, has been eliminated. Also, by testing single crystals, the possibility of intergranular stresses, generated by anisotropic growth and required by some yielding creep models, has been eliminated. Finally, by examination of the crystal surface after deformation in reactor it was hoped to be able to determine the relative importance of glide during in-reactor creep.

2. Experimental Procedure and Results

A. Creep Data

Three tensile specimens, each having a gauge length of about 2.4×10^{-2} m and a diameter of 3.2×10^{-3} m were spark machined from a single crystal of crystal-bar zirconium. The Schmidt factor for the most highly stressed $(10\bar{1}0)$ prism plane was 0.486. Two specimens

were reserved for in-reactor testing and the third was tested in the laboratory at 300°C at a stress of 25 MPa. On loading, the crystal deformed 15.5%. Over the next 100 hours the specimen accumulated an additional 0.5% strain, at a continually decreasing strain rate. For times greater than 100 hours the creep rate was immeasurably low.

The first in-reactor specimen was irradiated at a temperature of 300°C in a fast (> 1 MeV) neutron flux of 4.8×10^{16} n/m²·s (5.0×10^{-9} dpa/s) for 3600 hours at a stress of 1.5 MPa, the minimum stress required to maintain alignment of the creep rig. At the end of this time the fluence after allowing for shutdown time was 4.3×10^{23} n/m² (≈ 0.045 dpa). It was expected that the dislocation loop density would be near (within a factor of 3) its saturation level⁽¹¹⁾. No growth measurements were obtained during the pre-irradiation time period. The specimen was then loaded to 25 MPa with the reactor at full power; the resulting creep curve is shown in Fig. 1. After a loading strain of less than 0.1%, there was a period of primary creep lasting for about 20 hours. The creep rate after 20 hours was 5×10^{-6} h⁻¹. Fig. 2 shows the creep curve for the complete test. The portions of the curve obtained during shutdowns are offset from those obtained at full power because of the thermal expansion of the test rig. By the end of the test, the in-flux creep rate had decreased to 1.4×10^{-6} h⁻¹. During shutdowns the creep rate decreased rapidly to less than 5×10^{-7} h⁻¹.

The second in-reactor specimen was irradiated at 300°C, in

4.

a fast flux of 8.2×10^{16} n/m²·s (roughly twice that of the first test) at a very low stress of 5.8 MPa for 1360 hours. At the end of this time the total fluence had reached 3.3×10^{23} n/m² (\approx 0.035 dpa) or about 75% of that achieved with the first specimen. During the later stages of the test the creep rate was about 1×10^{-6} h⁻¹ with the reactor at power, and less than 5×10^{-7} h⁻¹ with the flux off. The specimen was loaded to 25 MPa during a long reactor shutdown; the creep curve, including some of the low stress data, is shown in Fig. 3. As for the first specimen there was a period of primary creep. After 20 hours the creep rate had decreased to 2.5×10^{-6} h⁻¹, or about half that observed in the first specimen which was loaded with the reactor at full power. When the reactor was brought to full power, the creep rate was observed to increase and achieve a nearly constant value. Fig. 4 shows the effect of a long shutdown from full power. The data have been corrected for thermal expansion of the creep rig. Before and after the shutdown the creep rate was about 3.4×10^{-6} h⁻¹; during the shutdown the rate decreased to less than 2×10^{-7} h⁻¹. There is some evidence of a small strain step occurring during the shutdown.

The test is still in progress and the flux enhanced creep rate has decreased slightly.

These tests conclusively show that there is a flux enhancement of creep in zirconium single crystals. The creep rate decreases slowly with time for at least the first 2000 hours for crystals that have been pre-irradiated to a dose of 4×10^{23} n/m² (\approx 0.04 dpa). The creep rates increase roughly linearly with both stress and flux, although precise stress and flux dependencies

cannot be determined from the present experiments.

A summary of test conditions and creep results is given in Table I.

TABLE I

	Rx-59	Rx-59B
gauge length	2.40×10^{-2} m	2.46×10^{-2} m
diameter	3.20×10^{-3} m	3.17×10^{-3} m
average fast (> 1 MeV) neutron flux	4.8×10^{16} n/m ² ·s (5×10^{-9} dpa/s)	8.0×10^{16} n/m ² ·s (8.4×10^{-9} dpa/s)
duration of test at low stress	3600 h (at 1.5 MPa)	1360 h (at 5.8 MPa)
total dose at time of loading to 25 MPa	4.3×10^{23} n/m ² (0.045 dpa)	3.3×10^{23} n/m ² (0.035 dpa)
creep rate at low stress	-	1×10^{-6} h ⁻¹
creep rate 20 h after loading to 25 MPa	5×10^{-6} h ⁻¹ (flux on)	2.5×10^{-6} h ⁻¹ (flux off)
creep rate near end of test	1.4×10^{-6} h ⁻¹ (flux on) < 5×10^{-7} h ⁻¹ (shutdown)	3.4×10^{-6} h ⁻¹ (flux on) < 2×10^{-7} h ⁻¹ (shutdown)
duration of test	5700 h (test complete)	2400 h (test still in progress)
total creep strain (post irradiation measurement)	0.6%	-

B. Microstructures

The first creep specimen was removed from the reactor after a total dose of 7.8×10^{23} n/m². It was observed that the gauge length was uniformly covered with very coarse slip lines.

Thin foils were prepared from sections cut parallel and normal to the slip plane, and were examined in a Phillips EM-300.

The microstructure in the slip plane is shown in Fig. 5. It is seen that the visible damage consists entirely of small loops. Network dislocations were only rarely visible. A histogram of the loop sizes for the area in Fig. 5 is given in Fig. 6. The loop number density is $4.5 \times 10^{26} \text{ m}^{-3}$, with an average loop size of 13.5 nm. The microstructure, and histogram of loop sizes in a section normal to the slip plane, are shown in Fig. 7 and 8. It is seen that both the loop density and average diameter are essentially the same as observed in a section containing the slip plane. Quantitative microscopy has not yet been completed, consequently it is not possible to define either the Burgers' vector or the character of the loops. A low magnification micrograph of an area normal to the slip plane, shown in Fig. 9, reveals a most interesting feature of the microstructure. Cleared swaths have formed during the creep deformation. Trace analysis confirms that the cleared channel is the trace of a primary, $(10\bar{1}0)$, prism plane. Fig. 10 shows the channel at a higher magnification.

Clearly, some irradiation damage exists within the channel. These loops could be a result of either the glide dislocations removing only some of the damage, or new loops having formed within the swept out region. The latter possibility, if true, would conclusively establish that the swaths formed during the creep deformation. Alternatively, one must consider the possibilities that the swaths formed on initial loading or accidentally when the specimen was removed from the creep rig. Both the small loading strain and the low loop density within the channels are inconsistent with the swaths forming when the specimen was first loaded. The uniform

distribution of slip lines over the entire gauge length of the specimen would seem to indicate that the specimen was not accidentally deformed. Thus it is concluded that the cleared channels formed by the passage of glide dislocations during the creep deformation. Glide dislocations would not be observed within the channels since $g \cdot b = 0$. For the areas that have been examined, roughly one swath per thinned area ($\approx 20 \mu\text{m}^2$) has been observed, and each had the general appearance shown in Fig. 9 and 10.

5. Discussion

A. Loops

The contribution from loop growth to the total strain rate has been calculated from the steady-state solutions to the rate equations for irradiation produced point defects. The point defect sinks were taken to be a dislocation loop density of $5 \times 10^{20} \text{ m}^{-3}$, as observed experimentally, and a network dislocation density of $2 \times 10^{10} \text{ m}^{-2}$. It is assumed that there were equal densities of edge and screw dislocations in the network. Only the screw dislocations can be considered to be neutral sinks. However, their low density means that, effectively, the crystal contains only one type of sink: edge dislocations, present primarily as prismatic loops. The calculations have been done in three ways, depending on the expression chosen for the bias factor of a prismatic loop. Heald and Speight⁽¹⁾, and Bullough and Hayns⁽⁴⁾ consider that loops can be treated analogously to straight edge dislocations, and thus the interaction energy between an isolated point defect and a straight edge, as

calculated by Bullough and Willis⁽¹²⁾, is used to calculate the bias factor. No distinction is made between vacancy and interstitial loops. The bias factor derived by Heald and Speight⁽¹⁾ has the form generally given in the literature,

$$Z = \frac{2\pi}{\ln(R/r_c)}$$

where R is half the distance between dislocations, and r_c is an effective capture radius. The expression for r_c depends on the alignment of the dislocation Burgers' vector with respect to the applied stress, and on the misfit strain and local elastic constants of the point defect. Thus there are four expressions for r_c representing the capture of vacancies or interstitials by either aligned (Burgers' vector parallel to the tensile stress) or non-aligned dislocations.

Bullough⁽¹³⁾ considers the logarithmic dependence on the dislocation spacing to be incorrect, and in the derivation of Bullough and Hayns⁽⁴⁾ the dislocation bias factors are given by expressions of the form:

$$Z = Z^0 [1 + f(\Delta G, \Delta K)]$$

Z^0 is the stress free bias factor which arises primarily from the misfit interaction between the dislocation and the point defect, and is considered to be a constant. For the present calculations Z_i^0 and Z_v^0 , the zero stress bias factors for interstitials and vacancies respectively, have been chosen to be 1.02 and 1.00. The expressions for f , like those for the capture radii, depend on the alignment of

the dislocation and on the local change in the shear and bulk moduli, ΔG and ΔK , caused by the point defect.

The calculations have been done using material parameters appropriate to zirconium, and with the temperature, stress, and flux of the experiment. It has been assumed that the interstitial is soft in shear, and that the vacancy has no effect on the shear modulus⁽¹⁻⁴⁾. A variety of loop distributions has been employed. For a random distribution and zero stress both the Heald and Speight and the Bullough expressions predict equal fluxes of vacancies and interstitials to the loops, and thus a zero strain rate. With a stress of 25 MPa both derivations give a slightly higher bias for aligned loops than for non-aligned loops. One then finds that aligned loops receive a net excess of interstitials, and non-aligned loops a net excess of vacancies. Thus, even though both aligned and non-aligned loops have a positive bias for interstitials, the fact that the bias of the non-aligned loops is smaller than that of the aligned loops, and the fact that there are no other sinks with a lower bias present, results in interstitial loops growing on aligned planes and vacancy loops growing on non-aligned planes. The strain rate in the direction of the applied stress calculated from Bullough's expression is $4 \times 10^{-10} \text{ h}^{-1}$. The Heald and Speight expression gives a rate of $1.8 \times 10^{-10} \text{ h}^{-1}$, about a factor of two lower than Bullough's.

Calculations have also been done assuming that 90% of the loops have aligned Burgers' vectors. With zero stress the result using Bullough's bias expression is, as for a random distribution, a zero strain rate. The Heald and Speight calculation, however, gives

a strain rate of $3 \times 10^{-8} \text{ h}^{-1}$. This result is a consequence of the bias factor depending inversely on the logarithm of the distance between dislocations. With a stress of 25 MPa the strain rate resulting from the growth of the loops is $1.6 \times 10^{-10} \text{ h}^{-1}$ using Bullough's bias, and $3 \times 10^{-8} \text{ h}^{-1}$ using the Heald and Speight expression. It is seen that using Bullough's bias expression the strain rate is lower with 90% alignment of the loops than for a random distribution. This is a result of the specimen approaching the conditions of having only one type of sink: aligned edge dislocations. For a single sink there can be no partitioning of the point defects and thus a zero strain rate would result.

Alternatively, one can calculate the bias factors for loops using the strain field of an infinitesimal dislocation loop, as done by Wolfer and Ashkin⁽²⁾. Using the corrected version of their calculation⁽¹⁴⁾, it is found that the loop bias factors for 6.5 nm radius loops are so small that no significant partitioning of the point defects can occur. Calculations done for a variety of assumed loop types and distributions all gave strain rates less than $3 \times 10^{-11} \text{ h}^{-1}$.

It is evident that the steady-state strain rates calculated for the microstructure observed and using the test conditions of the experiments are at least two to three orders of magnitude lower than observed experimentally. Thus one can conclude that the strain rate resulting directly from the growth of the prismatic loops is not a significant portion of the observed creep rate.

B. Cleared Swaths

Lacking detailed information on the slip band spacing and step height, one can only estimate the frequency of band formation that could give the observed creep rate. The shear strain in slip swaths in Cu, for swaths 100 nm wide, as in the present specimen, has been measured by Howe⁽¹⁵⁾ to be about 5. Taking this value as applicable for zirconium it is found that the formation of only one swath every 6 or 7 hours would give the observed creep rate. At such a band formation rate, for the fluence of this experiment, one would expect about 300 slip lines on the gauge length, and a slip line spacing of about 80 μm . If the strain per band were as low as 1, one swath forming every 1 1/3 hours would give the observed rate, and result in a slip line spacing of about 15 μm . The observation that on average only one swath was seen in each thinned area is in agreement with the expected slip line spacing.

C. Model for Swath Formation

For swath formation to be a viable mechanism for in-reactor creep, there must be a way for irradiation to allow swath formation at stresses below that required for swaths to form in the absence of flux. One possibility is as follows.

It has been shown above that in the absence of any sinks other than prismatic loops, the irradiation produced point defects will be partitioned such that aligned interstitial, and non-aligned vacancy loops will grow. However, the presence of another strong sink, having either a higher or lower bias than the loops, can perturb the balance and cause one type of loop to shrink. At the front of an

advancing swath there will be locally a high glide dislocation density. It seems reasonable to assume that the bias of a relatively straight edge dislocation will be greater than that of a small prismatic loop since the long range strain fields of the latter tend to cancel. Therefore, it is suggested that a group of edge dislocations, emitted from the same source and held up by the prismatic loops, will absorb a net excess of interstitials, and both types of prismatic loops, because of their lower bias, will receive a net flux of vacancies. Thus at the edge side of an expanding glide loop the local sink strengths will be altered such that interstitial loops will shrink and either disappear or at least become less effective obstacles to glide. Similarly an array of screw dislocations would be expected to act as a strong neutral sink causing the prismatic loops near them to receive a net interstitial flux. Thus on the screw side of an expanding swath one would expect the vacancy loops to shrink. Thus one can envision a slow swath formation controlled by the diffusion of point defects to the local dislocation configuration at the swath front. Whether or not the swath eventually becomes unstable and propagates rapidly across the crystal will depend on the rate at which the dislocation source emits new glide loops and the rate at which prismatic loops reform in the cleared channel.

4. Conclusions

1. Irradiation enhanced creep occurs in zirconium single crystals.
2. It is unlikely that the growth of the prismatic loops contributes significantly to the overall steady-state creep rate.

3. Cleared swaths, formed during the creep process, have been observed. It is thought that these are the major source of the creep strain.
4. A model has been suggested for flux enhanced swath formation.

Acknowledgements

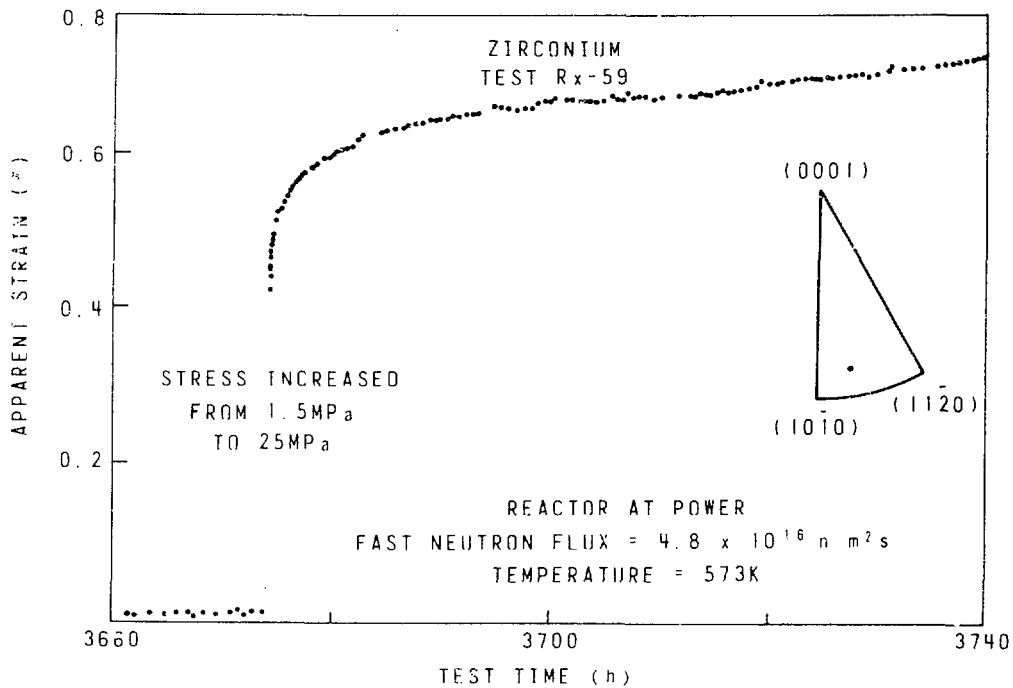
We wish to acknowledge the excellent technical assistance provided by I. Emmerton, in building the in-reactor creep rig, and J. Watters in preparing specimens for electron microscopy. Discussions with L.M. Howe and R. Bullough are gratefully acknowledged.

References

1. P.T. Heald and M.V. Speight, Acta. Met. 23, 1389 (1975).
2. W.G. Wolfer and M. Ashkin, J.A.P. 46, 547 (1975).
3. W.G. Wolfer, Scripta Met. 9, 801 (1975).
4. R. Bullough and M.R. Hayns, J Nucl. Mater. 57, 348 (1975).
5. F.A. Nichols, J. Nucl. Mater. 30, 249, (1969)
6. C.C. Dollins, Rad. Effect 11, 123 (1971).
7. C.C. Dollins, and F.A. Nichols, Spec. Tech. Publ. 551. American Soc. for Testing and Materials, p.229 (1974).
8. J.H. Gittus, Phil. Mag. 25, 345 (1972).
9. J.H. Gittus. Phil. Mag. 30, 751 (1975).
10. R.V. Hesketh, J. Nucl. Mater. 26, 77 (1968).
11. D.O. Northwood, unpublished results.
12. R. Bullough and J.R. Willis, Phil. Mag. 31, 855 (1975).
13. R. Bullough, private communication.
14. W.G. Wolfer and H. Ashkin, J.A.P. 46, 4108 (1975).
15. L.M. Howe, Rad. Effects, 23, 181 (1974).

Figure Captions

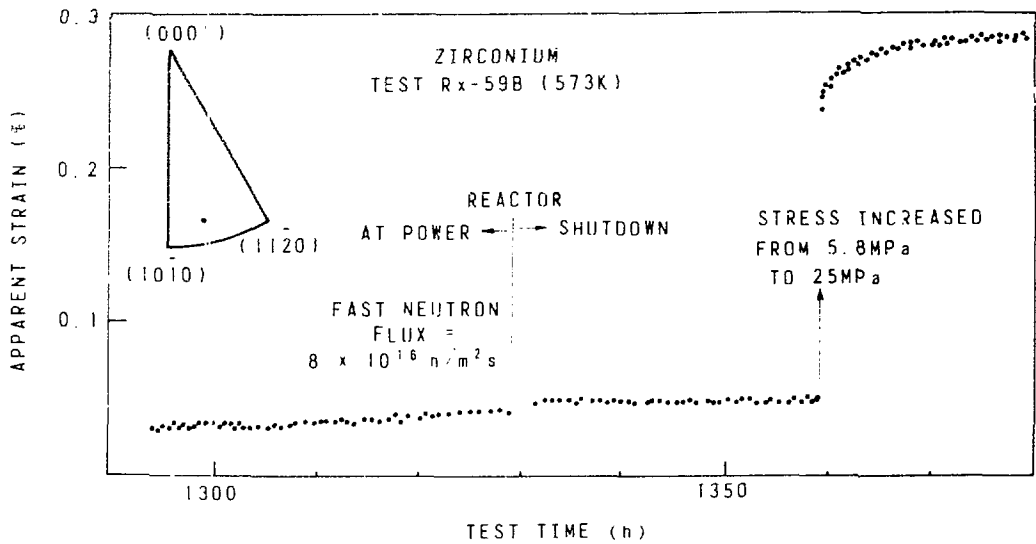
1. Initial portion of Rx-59 creep curve at 25 MPa.
2. Complete Rx-59 creep curve at 25 MPa.
3. Latter stages of the low stress creep curve for Rx-59(B) and the initial primary creep caused by loading to 25 MPa.
4. Flux effect in Zr single crystal demonstrated by a long shutdown during test Rx-59(B).
5. Irradiation produced dislocation loops in a section containing the primary slip plane. (X93,000)
6. Histogram of the loops size distribution for the loops of Fig. 5.
7. Irradiation produced dislocation loops in a section cut normal to the primary slip plane. (X93,000)
8. Histogram of the loop size distribution for the loops of Fig. 7.
9. Low magnification micrograph of a section cut normal to the slip plane of the creep specimen of test Rx-59. The cleared swaths are traces of $(10\bar{1}0)$ planes. (X11,000)
10. High magnification micrograph of a swath showing damage reforming within the cleared channel. (X93,000)



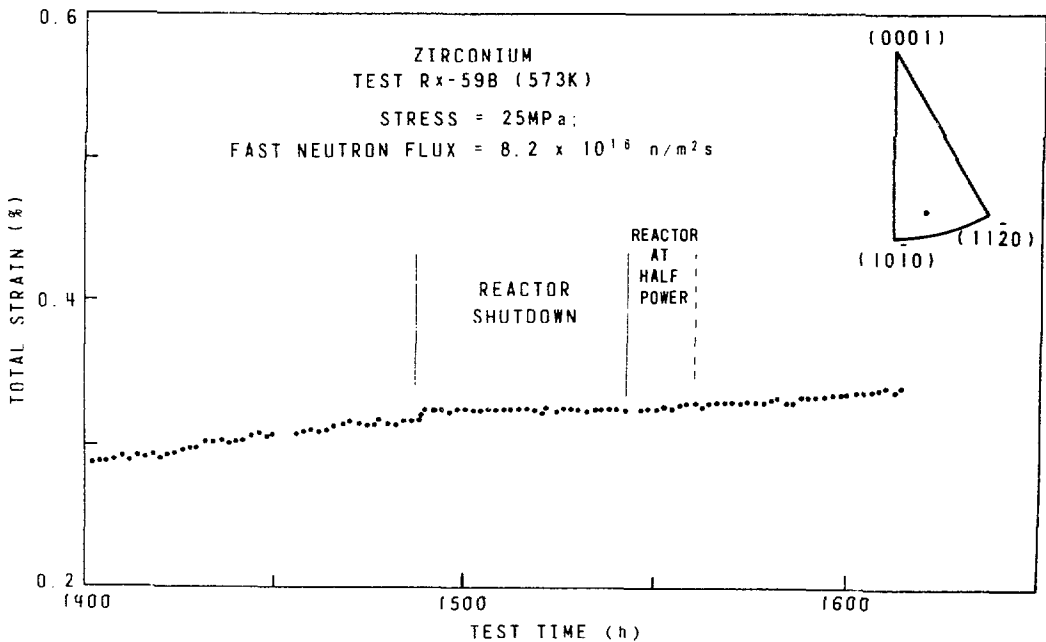
Initial portion of Rx-59 creep curve at 25 MPa. FIG. 1



Complete Rx-59 creep curve at 25 MPa. FIG. 2



Latter stages of the low stress creep curve for Rx-59(B) and the initial primary creep caused by loading to 25 MPa. FIG. 3



Flux effect in Zr single crystal demonstrated by a long shutdown during test Rx-59(B). FIG. 4

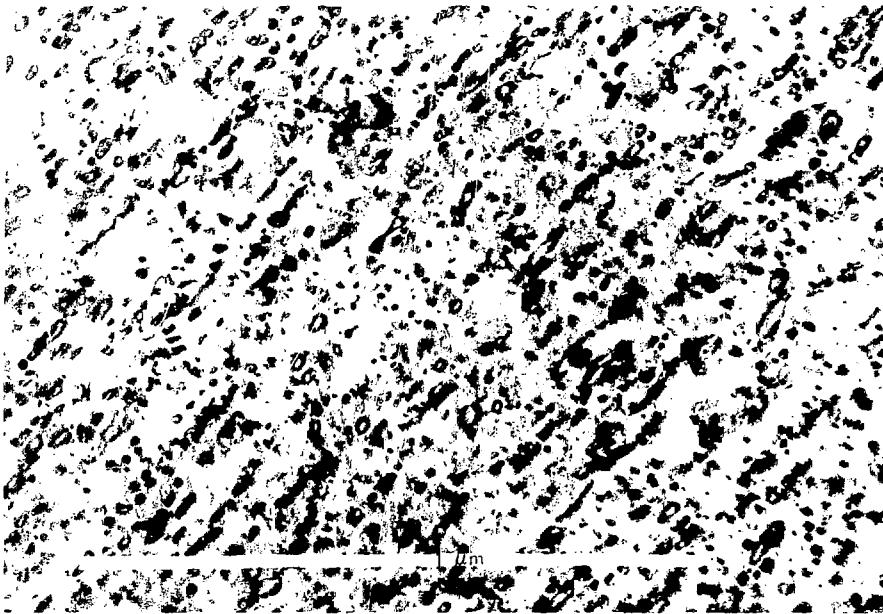


FIG. 5

Irradiation produced dislocation loops in a section containing the primary slip plane. (X93,000)

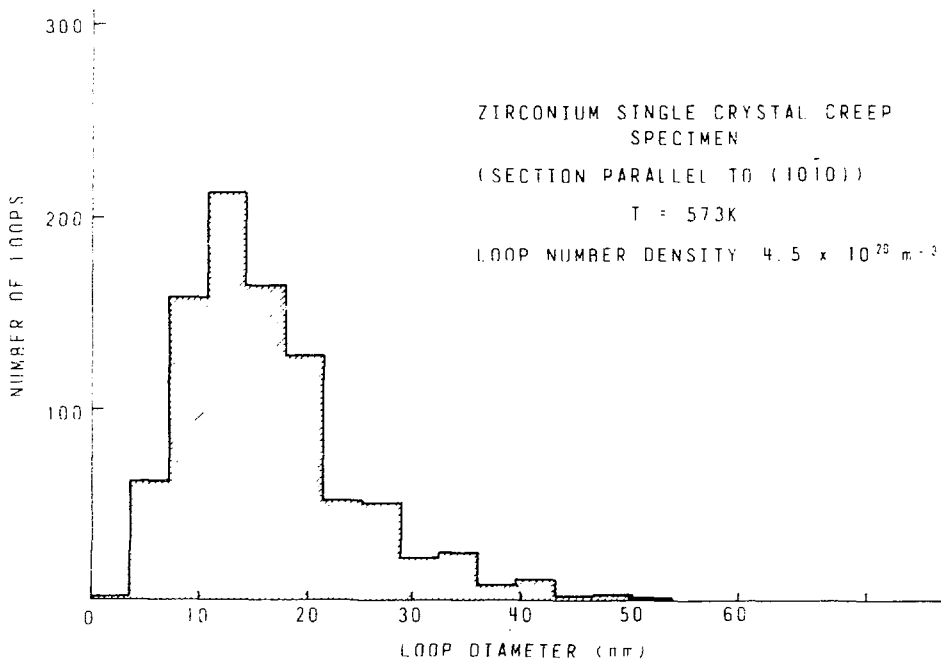


FIG. 6

Histogram of the loops size distribution for the loops of Fig. 5.

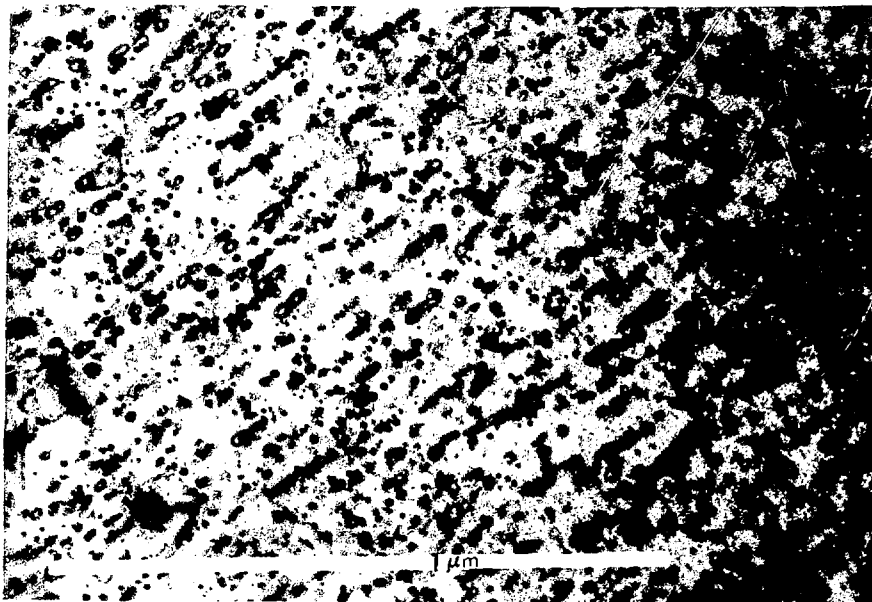


FIG. 7

Irradiation produced dislocation loops in a section cut normal to the primary slip plane. (X93,000)

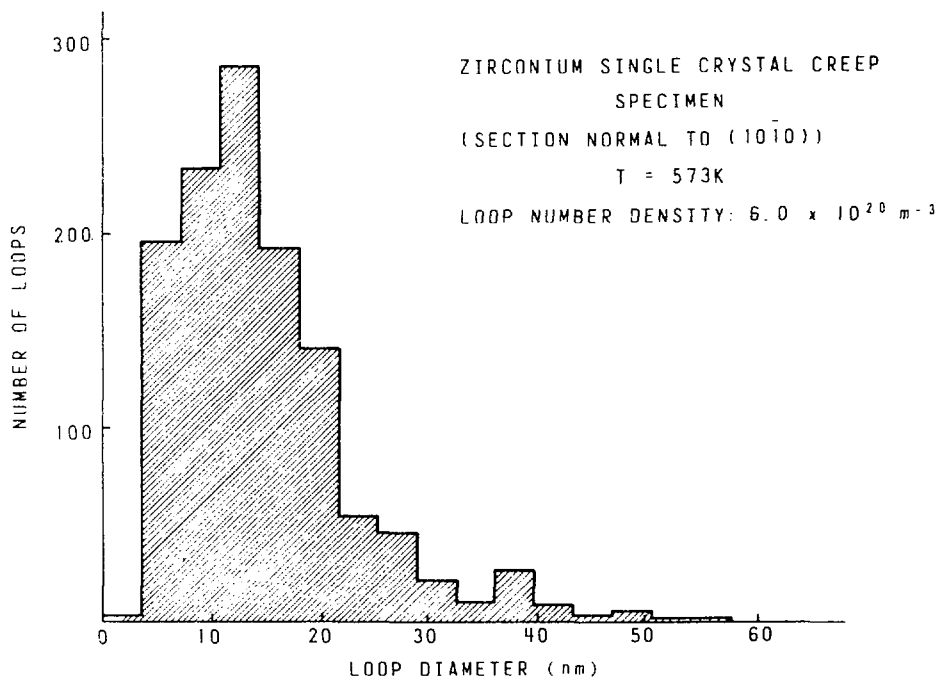


FIG. 8

Histogram of the loop size distribution for the loops of Fig. 7.

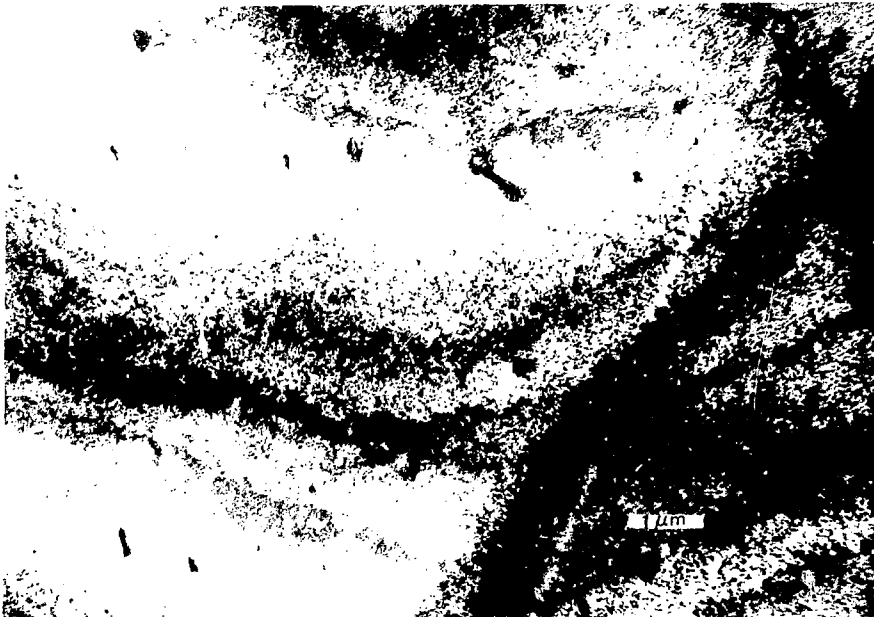


FIG. 9

Low magnification micrograph of a section cut normal to the slip plane of the creep specimen of test Rx-59. The cleared swaths are traces of (1010) planes. (X11,000)

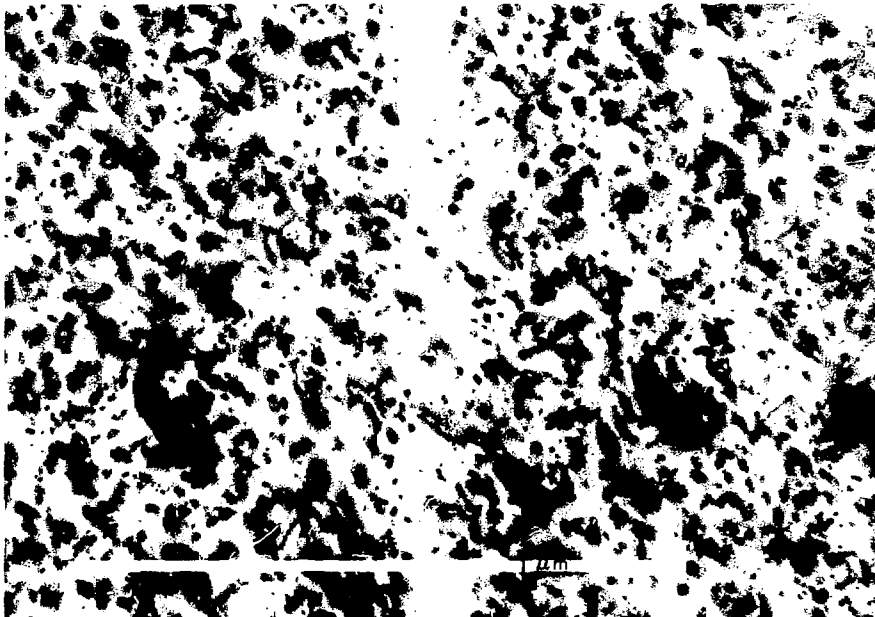


FIG. 10

High magnification micrograph of a swath showing damage reforming within the cleared channel. (X93,000)



The International Standard Serial Number

ISSN 0067-0367

has been assigned to this series of reports.

**To identify individual documents in the series
we have assigned an AECL-number.**

**Please refer to the AECL-number when
requesting additional copies of this document
from**

**Scientific Document Distribution Office
Atomic Energy of Canada Limited
Chalk River, Ontario, Canada**

K0J 1J0

Price \$3.00 per copy

1300-76